CHAPTER IV
RESULTS AND DISCUSSION

In the Yuan *et al.* (2009) study, the hydrotalcite (HT), MgO, Al_2O_3, H-ZSM5, and H-Beta supported Pt catalysts were prepared and tested for hydrogenolysis of glycerol to propylene glycol. They found that the solid base such as hydrotalcite and MgO supported Pt catalysts exhibited the predominant activity and higher propylene glycol selectivity than the Pt supported solid acid such as Al_2O_3, H-ZSM5 and H-Beta catalysts. Therefore, in the present study, four CuZnO supported catalysts, CuZnO/MgO, CuZnO/HT, CuZnO/Al_2O_3, and CuZnO/ASA catalysts, were prepared and tested for their activity.

4.1 Fresh Catalyst Characterization

4.1.1 Brunauer–Emmett–Teller Method (BET)

Textual properties (surface area, total pore volume, and mean pore diameter) of the supports and the catalysts were obtained from the Brunauer–Emmett–Teller surface area analyzer are shown in Table 4.1. The surface area of Al_2O_3, ASA, MgO, and HT were 253, 426, 168, and 25 m^2/g, respectively. The surface area of CuZnO/Al_2O_3, CuZnO/ASA, CuZnO/MgO, and CuZnO/HT were 121, 71, 24, and 24 m^2/g, respectively. In addition, the pore size distribution curves of the supports and the catalysts are shown in Figure 4.1. The results showed that pore volume of the catalysts were less than that of the supports and the small pores of CuZnO/ASA were very less than its supports. The surface area and pore volume of the catalysts were lower than those of the supports. This could be due to the high amount of metal loading that could plug the pore of the supports.

The kinetic diameter of glycerol is 0.63 nm (Dimian, 2012). The CuZnO-based catalysts with different catalyst supports have different pore sizes, as shown in Table 4.1. The pore diameter of CuZnO/Al_2O_3, CuZnO/ASA, CuZnO/MgO, and CuZnO/HT were 8.84, 8.78, 0.97, and 3.6 nm, respectively. The kinetic diameter of glycerol is smaller than all of the prepared catalysts. Thus, the reactions can occur inside the pores.

Table 4.1 BET surface area, pore volume, and pore size diameter of the supports and the catalysts

Property	$CuZnO/Al_2O_3$		CuZnO/ASA		CuZnO/MgO			CuZnO/HT	
	Support	Catalyst	Support	Catalyst	Support	Catalyst	Regenerated catalyst	Support	Catalyst
Surface area (m^2/g)*	253	121	426	71	168	24	31	25	24
Pore volume (cc/g)*	0.87	0.36	0.63	0.17	0.36	0.18	0.16	0.23	0.23
Pore diameter (nm)*	8.76	8.84	4.69	8.78	0.97	0.97	3.66	3.6	3.6

* calculated using BjH method

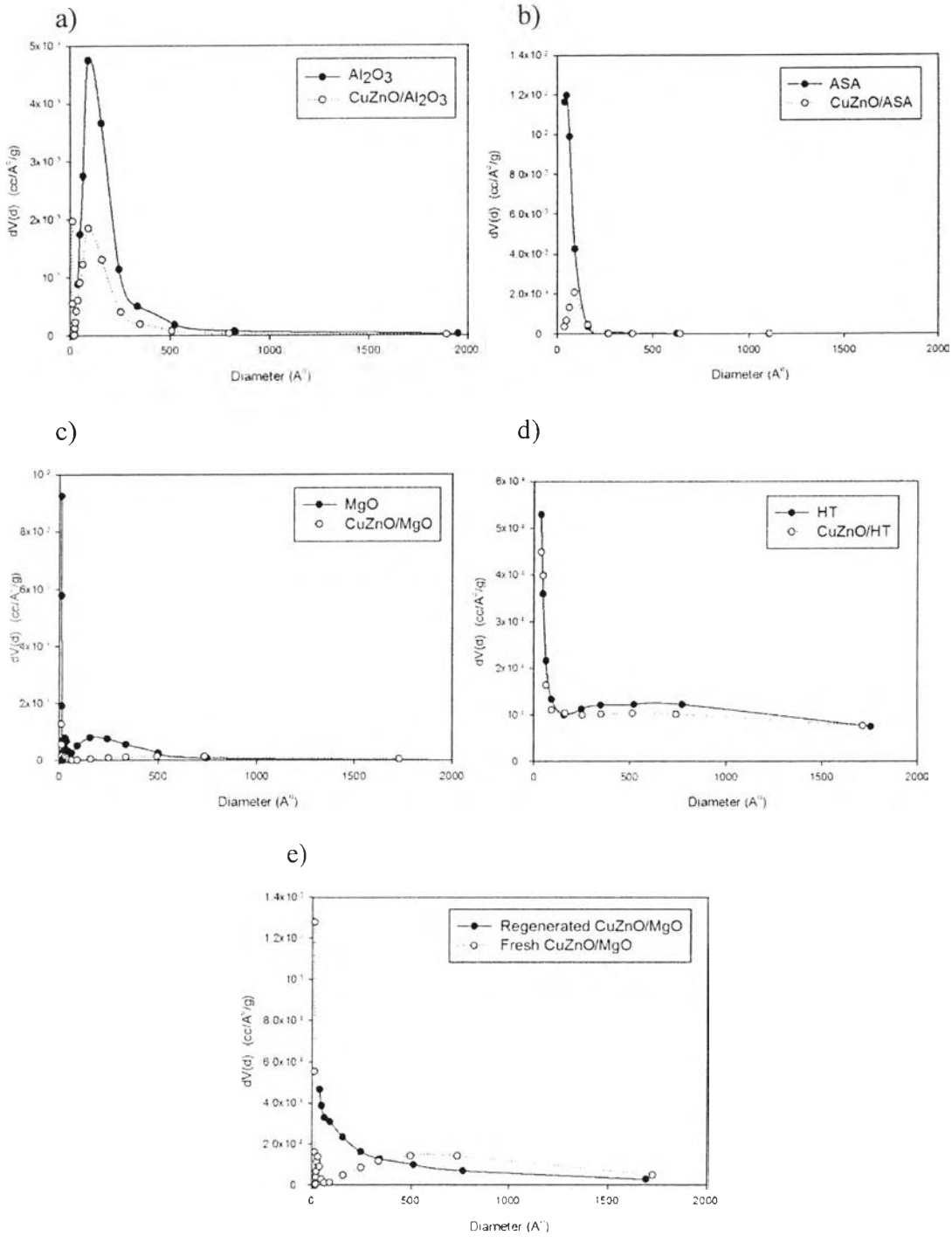

Figure 4.1 Pore size distribution of different catalysts compared to its support obtained for the supports and the catalysts a) $CuZnO/Al_2O_3$, b) CuZnO/ASA, c) CuZnO/MgO, d) CuZnO/HT, and e) regenerated CuZnO/MgO.

4.1.2 X-ray Diffraction (XRD)

The XRD patterns of the CuZnO-based catalysts with different catalyst supports are illustrated in Figure 4.2. The XRD patterns of the $CuZnO/Al_2O_3$, CuZnO/ASA, CuZnO/MgO, and CuZnO/HT catalysts were quite similar, consisting of ZnO phases which appeared at 2θ of 31.9°, 34.4°, 36.3°, 47.6°, 56.6°, 62.7°, 65.7°, 68.2°, and 69.0° and CuO phases which appeared at 2θ of 35.6° and 38.8° with comparable peak intensity. Nevertheless, Cu_2O phase at 2θ of 36.8° was found only in CuZnO/MgO and MgO phases at 2θ of 42.9° and 62.3° were found in CuZnO/MgO and CuZnO/HT.

The intensity of CuO peak decreased in the following orders: CuZnO/HT > CuZnO/ASA > $CuZnO/Al_2O_3$ > CuZnO/MgO. The sharper and stronger of XRD peak indicated the high crystalline size of CuO or poor dispersion (Tang *et al.*, 2009). The crystallite sizes of CuO and MgO were calculated based on the Scherrer's equation and the results are summarized in Table 4.2.

The disappearance of free CuO in CuZnO/MgO might reflect the dissolution of CuO in MgO lattice. This facilitates the formation of CuO-MgO solid solution (El-Molla, 2005).

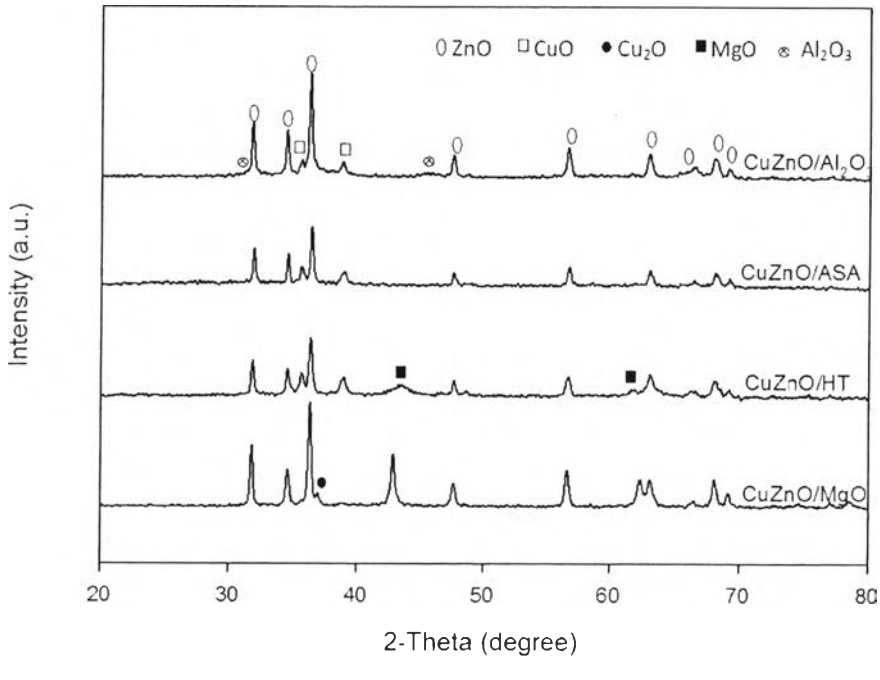

Figure 4.2 XRD patterns of the CuZnO-based catalysts with different catalyst supports.

Table 4.2 CuO and MgO crystallite sizes of the CuZnO-based catalysts with different catalyst supports

Catalysts	CuO Crystallite size (nm)	MgO Crystallite size (nm)
$CuZnO/Al_2O_3$	21.57	-
CuZnO/ASA	22.25	-
CuZnO/HT	23.80	13.44
CuZnO/MgO	ND*	27.33
Regenerated CuZnO/MgO	18.30	25.71

*ND cannot be detected via XRD

4.1.3 Temperature Programmed Reduction (TPR)

Figure 4.3 exhibits the TPR profiles of the CuZnO-based catalysts with different catalyst supports. A symmetric reduction peak appeared on $CuZnO/Al_2O_3$, with the lowest temperature, 239 °C, compared to CuZnO/ASA and CuZnO/HT at 265 and 286 °C, respectively. It was reported that the reduction temperature related to the size of CuO particle in $Cu/ZnO/ZrO_2$ catalysts. The higher reduction temperature could indicate the larger CuO particle (Gao *et al.*, 2011). Thus, the CuO particle size was obtained in the order of $CuZnO/Al_2O_3$ < CuZnO/ASA < CuZnO/HT.

The H_2-TPR profile consisting of a main peak at 253 °C and a small shoulder at 233 °C was observed on CuZnO/MgO. In addition, Cu_2O phase was found in CuZnO/MgO, as shown in Figure 4.1. Thus, those peaks are assigned to the reduction of CuO (Cu^{2+}) and Cu_2O (Cu^{1+}) species, respectively (Delahay *et al.*, 1997).

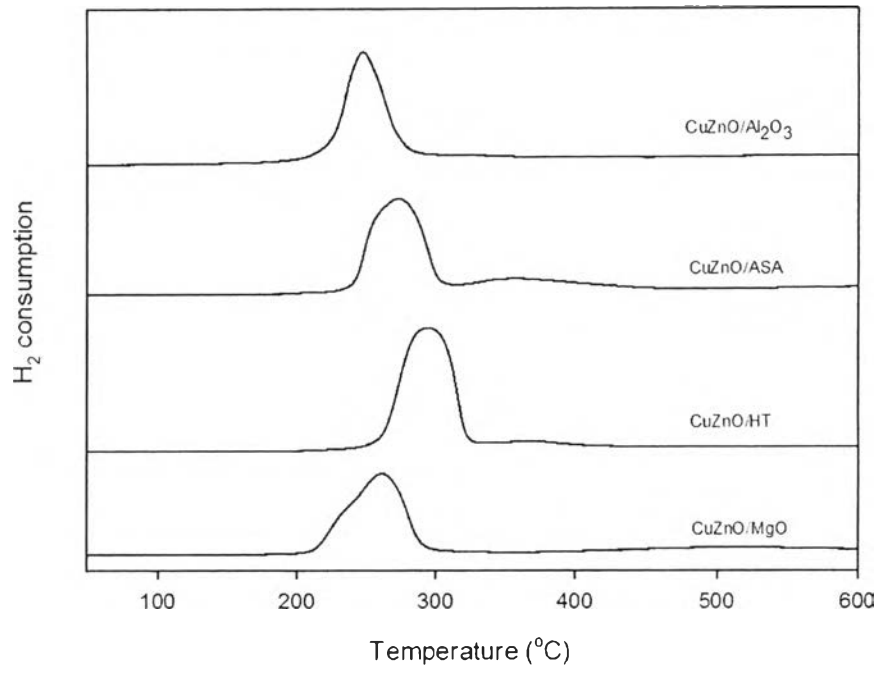

Figure 4.3 TPR profiles of the CuZnO-based catalysts with different catalyst supports.

4.1.4 Temperature Programmed Desorption of Carbon Dioxide (CO_2-TPD)

The CO_2-TPD technique is used for determining the surface basicity of the catalysts. Figure 4.4 illustrates the CO_2-TPD profiles of the different supported catalysts. In addition, the basicity of the prepared catalysts from TPD of CO_2 is summarized in Table 4.3.

There are three different desorption peaks which are 1) α peak (the weak basic site at ~130 °C), 2) β peak (the median basic site at ~210 °C), and 3) γ peak (the strong basic site at ~410 °C) (Li *et al.*, 2010).

It was implied that the higher amount of CO_2 desorbed would result from the higher basic sites of the catalyst. There are three desorption peaks (α, β, and γ) in $CuZnO/Al_2O_3$. CuZnO/ASA gave a diminutive desorption peak at γ position. CuZnO/MgO gave two desorption peaks at α and β positions. And CuZnO/MgO gave three desorption peaks at α, β, and γ positions. The results indicated that the weak basic site was in the order of $CuZnO/Al_2O_3$ > CuZnO/HT > CuZnO/MgO. The median basic site was in the order of $CuZnO/Al_2O_3$ > CuZnO/MgO. The strong basic

site was in the order of CuZnO/MgO > CuZnO/HT > CuZnO/Al_2O_3 ~ CuZnO/ASA. CuZnO/MgO had the highest total basicity and basic strength followed by CuZnO/HT, CuZnO/Al_2O_3, CuZnO/ASA, respectively.

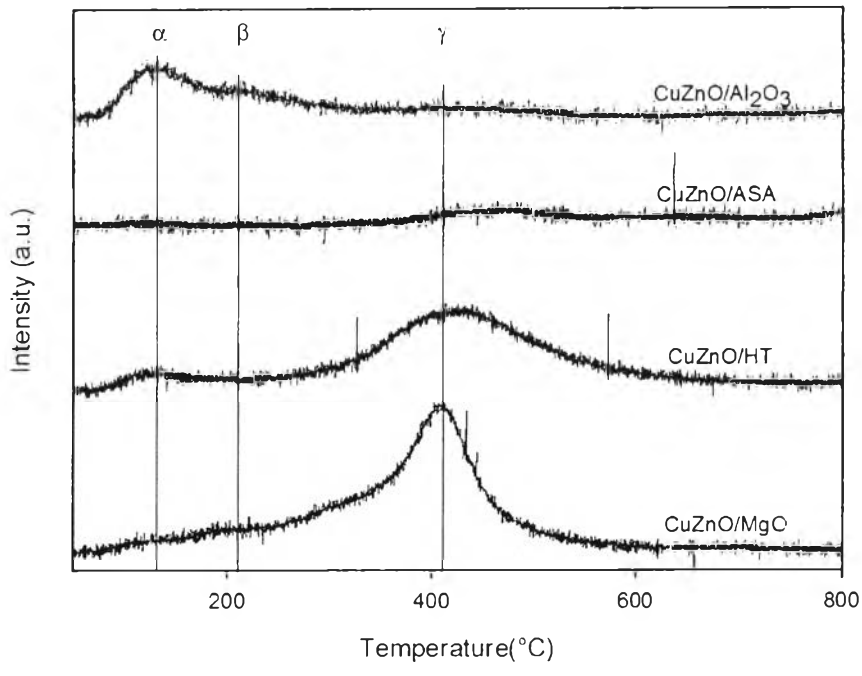

Figure 4.4 CO_2-TPD profiles of the CuZnO-based catalysts with different catalyst supports.

Table 4.3 Basicity of the prepared catalysts from TPD of CO_2

Catalysts	Basicity of catalysts (μmol/g)
CuZnO/Al_2O_3	7.01
CuZnO/ASA	4.10
CuZnO/HT	15.25
CuZnO/MgO	18.18

4.2 Catalytic Activity Testing

4.2.1 Effect of Catalyst Supports

The CuZnO prepared with different supported catalysts were tested for their catalytic performance in conversion of glycerol to propylene glycol. The plot of glycerol conversion, PG selectivity, and acetol selectivity are shown in Figures 4.5-4.7, respectively. The results show that $CuZnO/Al_2O_3$ gave the highest catalytic activity, followed by CuZnO/MgO, CuZnO/HT, and CuZnO/ASA, respectively. This could be due to the much higher surface area of $CuZnO/Al_2O_3$ compared to the other prepared catalysts. In addition, the catalytic activity could be due to the basicity of the prepared catalysts (Yuan *et al.*, 2009) which were obtained in the order of CuZnO/MgO > CuZnO/HT > $CuZnO/Al_2O_3$> CuZnO/ASA from the TPD-CO_2 results. As a result, the catalytic activity of CuZnO/MgO is higher than CuZnO/HT, and CuZnO/ASA, respectively. Noticeably, CuZnO/MgO exhibited the highest performance compared to the other prepared catalysts in terms of stability.

From Table 4.2, the crystalline size of MgO of the regenerated CuZnO/MgO catalyst was smaller than the fresh catalyst. This could be the reason that the glycerol conversion of fresh CuZnO/MgO slightly increased with time on stream.

From Figures 4.5-4.6, the decreasing of propylene glycol selectivity led to the increasing of acetol selectivity. The results well agreed with the mechanism proposed by Dasari *et al.* (2005), as shown in Figure 4.8.

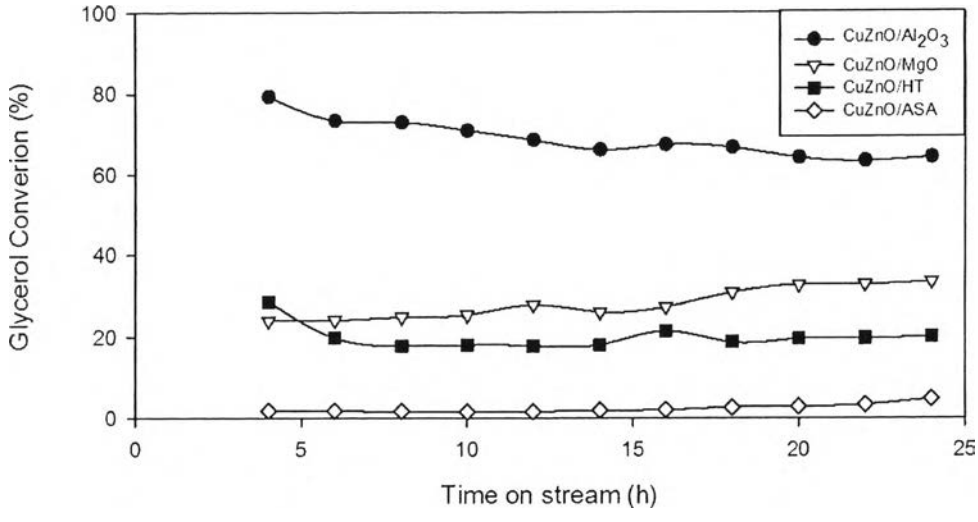

Figure 4.5 Plot of glycerol conversion as a function of time on stream the CuZnO-based catalysts at different catalyst supports (Reaction conditions: 80wt% glycerol feed, 250 °C, 500 psig, H_2:glycerol = 4:1, and WHSV = 3.77 h^{-1}).

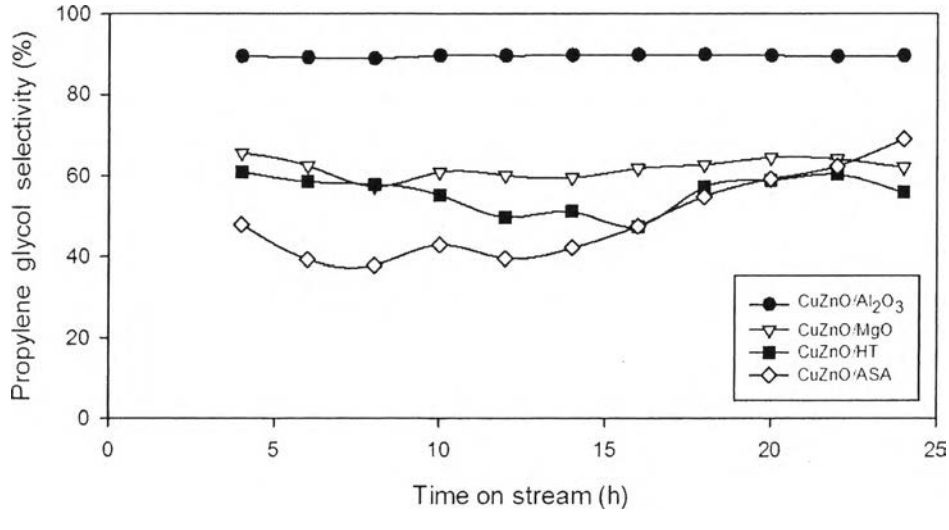

Figure 4.6 Plot of selectivity to propylene glycol as a function of time on stream with the CuZnO-based catalysts at different catalyst supports (Reaction conditions: 80wt% glycerol feed, 250 °C, 500 psig, H_2:glycerol = 4:1, and WHSV = 3.77 h^{-1}).

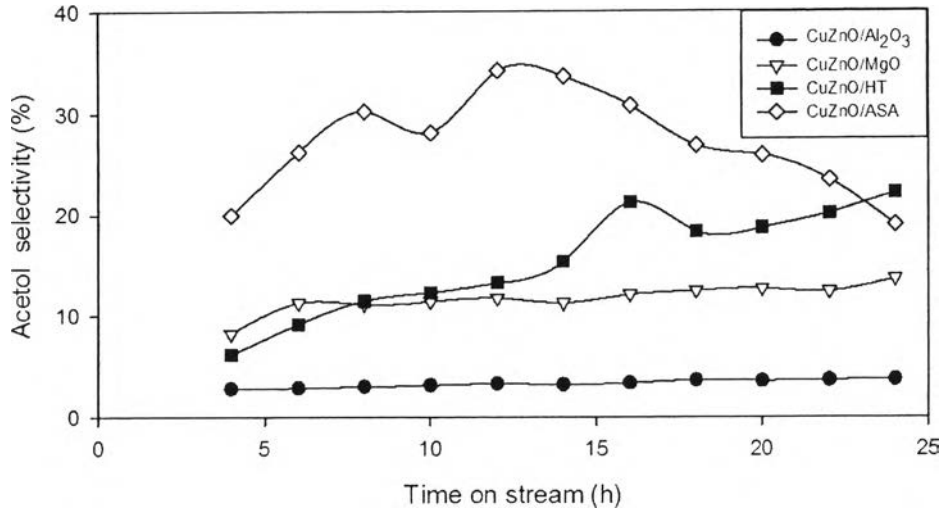

Figure 4.7 Plot of selectivity to acetol intermediate as a function of time on stream with the CuZnO-based catalysts at different catalyst supports (Reaction conditions: 80wt% glycerol feed, 250 °C, 500 psig, H_2:glycerol = 4:1, and WHSV = 3.77 h^{-1}).

Table 4.4 Conversion and selectivity to liquid products of the CuZnO-based catalysts with different catalyst supports (Reaction conditions: 80wt% glycerol feed, 250 °C, 500 psig, H_2:glycerol = 4:1, WHSV = 3.77 h^{-1}, and TOS of 24 h)

Catalysts		**$CuZnO/Al_2O_3$**	**CuZnO/ASA**	**CuZnO/MgO**	**CuZnO/HT**
Conversion (wt. %)		58.42	3.92	29.88	17.16
Selectivity to liquid products (wt. %)	Acetone	-	1.69	1.93	1.68
	2-propanol	0.67	-	0.99	-
	Acetol	3.65	18.88	9.78	16.26
	Propylene Glycol	88.43	68.56	64.29	59.06
	Ethylene Glycol	3.76	2.98	4.13	4.86
	Others	3.49	7.89	18.88	18.14

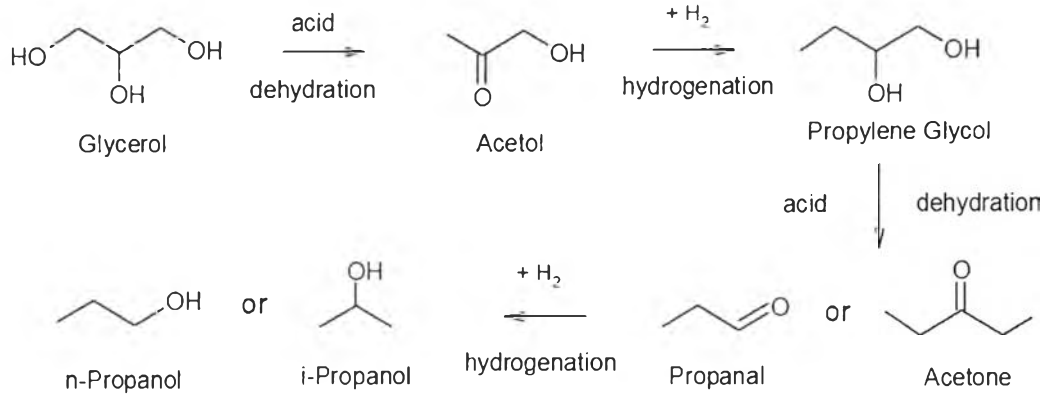

Figure 4.8 The glycerol conversion mechanism (Dasari *et al.*, 2005).

Figure 4.9 shows the TPO profiles and the percentages of carbon deposit on the spent CuZnO loaded on different support catalysts after 24 h TOS which analyzed by temperature programmed oxidation (TPO). It was found that the spent CuZnO/HT catalyst contained the highest amount of coke, followed by the spent CuZnO/MgO catalyst, the spent CuZnO/Al_2O_3 catalyst, and the spent CuZnO/ASA catalyst, respectively. Coke deposition might poison the active site of the catalysts, which lower the catalytic activity. Nevertheless, CuZnO/ASA had very low activity which led to very low coke formation.

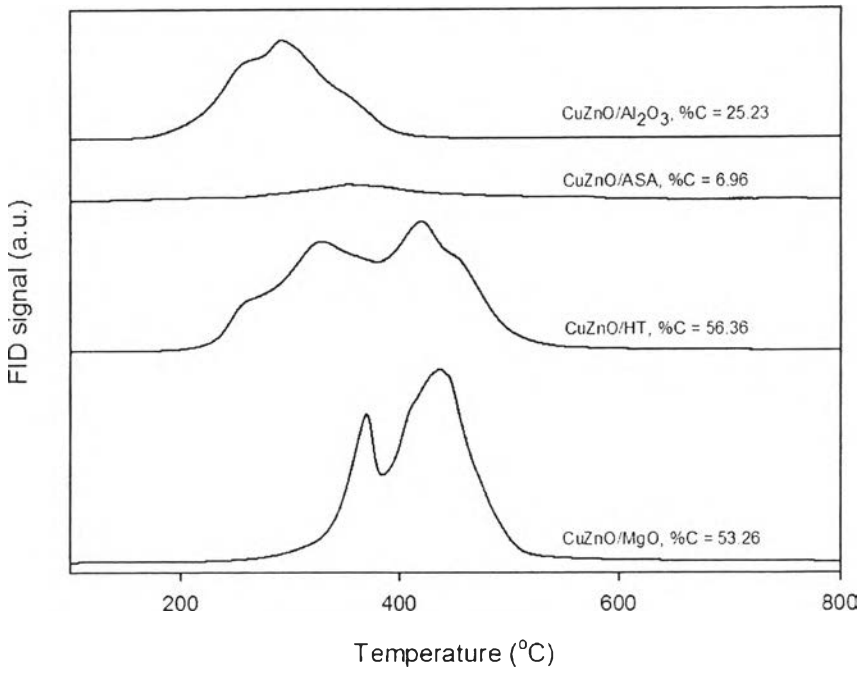

Figure 4.9 TPO profiles of the spent CuZnO-based catalysts with different catalyst supports after 24 h TOS (Reaction conditions: 80 wt% glycerol feed, 250 °C, 500 psig, H_2:glycerol = 4:1, and WHSV = 3.77 h^{-1}).

4.2.2 Effect of Alkali (Na, K) Addition in Feed

The previous study (Auttanat, 2012) concluded that the impurities (Na and K) contained in the refined glycerol lowered the catalytic activity of the dehydroxylation of glycerol to propylene glycol over $CuZnO/Al_2O_3$. Therefore, the two highest performance catalysts, $CuZnO/Al_2O_3$ and CuZnO/MgO, were selected to investigate for the effect of Na and K impurities contained in glycerol feedstock.

Figure 4.10 illustrates the graph of glycerol conversion as a function of time on stream over $CuZnO/Al_2O_3$ on different impurities in the glycerol feedstock—the refined glycerol, the refined glycerol mixed with 0.1% Na, and the refined glycerol mixed with 0.1% K. The results show that the refined glycerol exhibited the highest conversion, followed by the refined glycerol mixed with 0.1% Na and with 0.1% K, respectively. This could be because the Na and K might deposit on the catalysts, as shown in Table 4.6, and poison the active site of catalysts so that the conversion of glycerol decreased. The decrease of glycerol conversion was more

pronounced when the feed was contaminated with 0.1% K, as compared to the one contaminated with Na. This could be because the atom radius of K (220 pm) is higher than Na (190 pm) so K atom might block the pores of the catalyst easier than Na (Slater *et al.*, 1964).

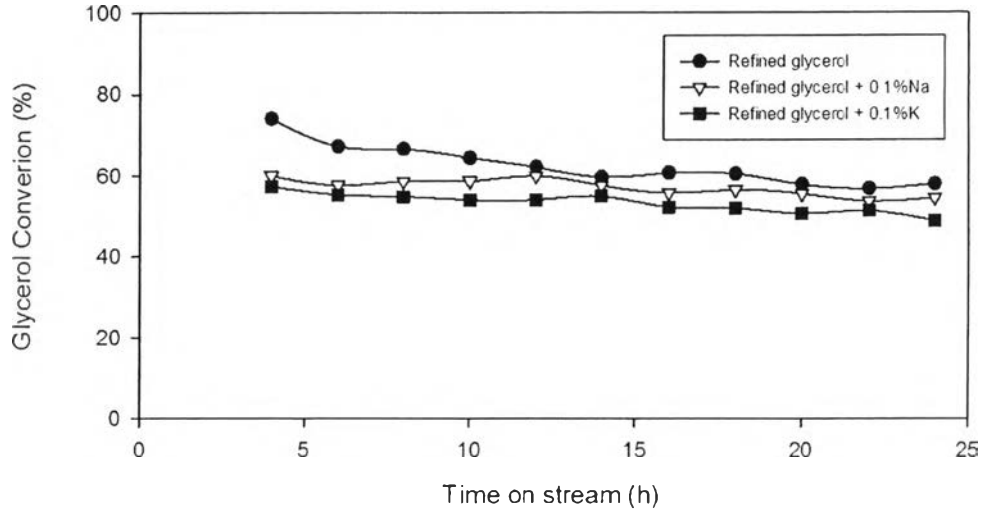

Figure 4.10 Plot of glycerol conversion as a function of time on stream over $CuZnO/Al_2O_3$ on different impurities in the glycerol feedstock (Reaction conditions: 80wt% glycerol feed, 250 °C, 500 psig, H_2:glycerol = 4:1, and WHSV = 3.77 h^{-1}).

Figures 4.11-4.12 show the propylene glycol selectivity and the acetol selectivity of $CuZnO/Al_2O_3$ on different impurities in the glycerol feedstock —the refined glycerol, the refined glycerol mixed with 0.1% Na, and the refined glycerol mixed with 0.1% K. The decreasing of propylene glycol selectivity led to the increasing of acetol selectivity. The results well agreed with the mechanism proposed by Dasari *et al.* (2005) as shown in Figure 4.8.

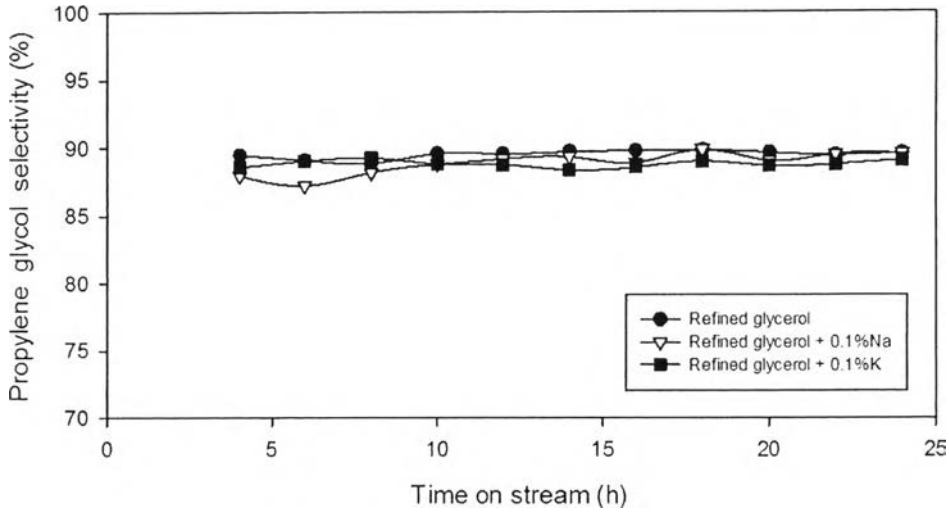

Figure 4.11 Plot of selectivity to propylene glycol as a function of time on stream over $CuZnO/Al_2O_3$ on different impurities in the glycerol feedstock (Reaction conditions: 80wt% glycerol feed, 250 °C, 500 psig, H_2:glycerol = 4:1, and WHSV = 3.77 h^{-1}).

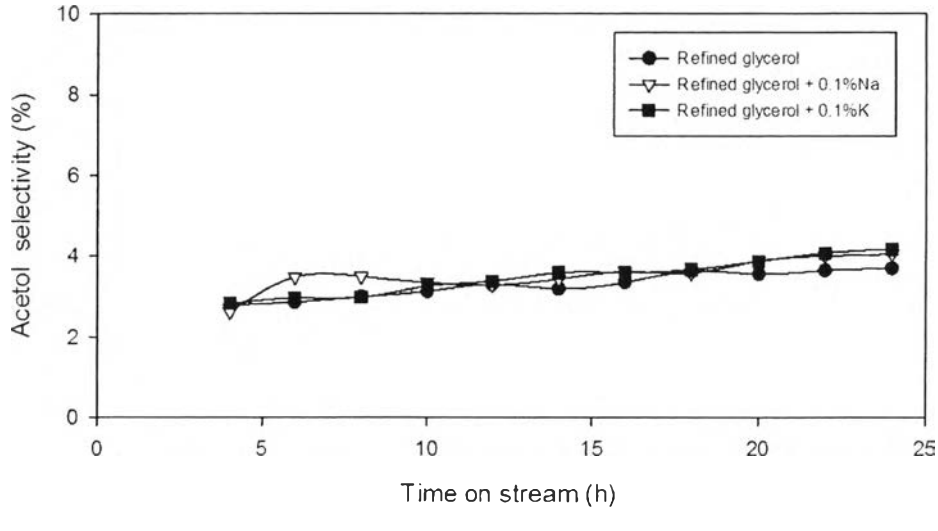

Figure 4.12 Plot of selectivity to acetol intermediate as a function of time on stream over $CuZnO/Al_2O_3$ on different impurities in the glycerol feedstock (Reaction conditions: 80wt% glycerol feed, 250 °C, 500 psig, H_2:glycerol = 4:1, and WHSV = 3.77 h^{-1}).

Table 4.5 Conversion and selectivity to liquid products of $CuZnO/Al_2O_3$ on different impurities in the glycerol feedstock (Reaction conditions: 80wt% glycerol feed, 250 °C, 500 psig, H_2:glycerol = 4:1, WHSV = 3.77 h^{-1}, and TOS of 24 h)

Catalysts		**Refined glycerol**	**Refined glycerol + 0.1%Na**	**Refined glycerol + 0.1%K**
Conversion (wt. %)		58.42	54.79	49.14
Selectivity to liquid products (wt. %)	2-propanol	0.67	-	-
	Acetol	3.65	4.00	4.12
	Propylene Glycol	88.43	88.36	87.55
	Ethylene Glycol	3.76	3.44	3.68
	Others	3.49	4.20	4.65

The TPO profiles and the calculated amounts of carbon deposition on the spent $CuZnO/Al_2O_3$ catalyst with different feedstocks—the refined glycerol, the refined glycerol mixed with 0.1% Na, and the refined glycerol mixed with 0.1% K are shown in Figure 4.13. The results show that the spent catalyst of the refined glycerol as feedstock contained the highest amount of coke compared to the spent catalyst of the refined glycerol mixed with 0.1% Na, and the refined glycerol mixed with 0.1% K. This could be because Na and K which contaminated in feedstocks poisoned the active site of the catalysts and led to lower catalytic activity and coke.

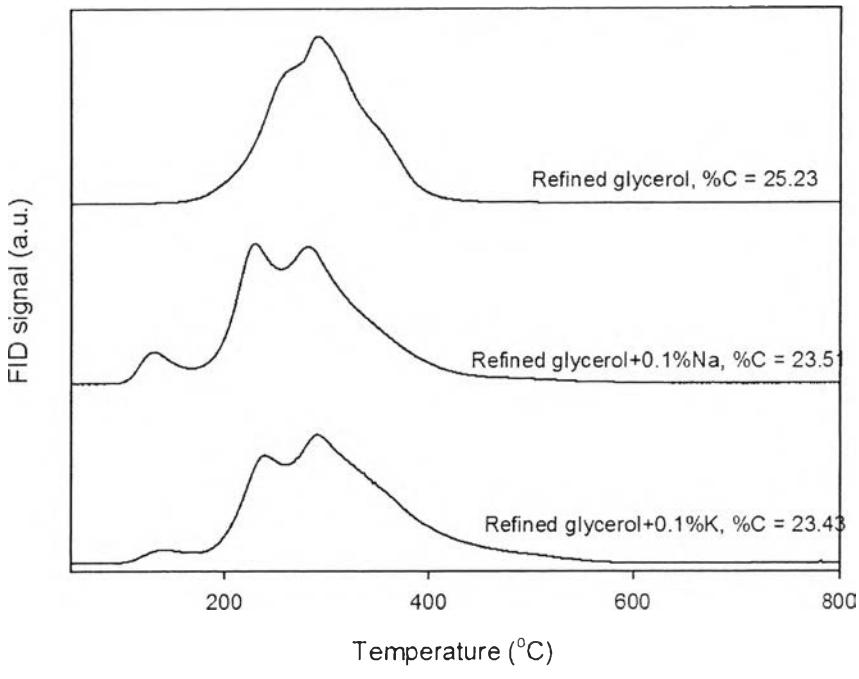

Figure 4.13 TPO profiles of CuZnO/ Al_2O_3 on different impurities in the glycerol feedstock after 24 h TOS (Reaction conditions: 80wt% glycerol feed, 250 °C, 500 psig, H_2:glycerol = 4:1, and WHSV = 3.77 h^{-1}).

Atomic absorption spectroscopy (AAS) was used to investigate the possibility of alkali which deposited on the spent CuZnO/Al_2O_3 and CuZnO/MgO catalysts, AAS. From Table 4.6, Na and K were deposited on CuZnO/Al_2O_3 but hardly deposited in the CuZnO/MgO. This could be because Na and K are base metals, CuZnO/MgO is the solid base catalyst, and CuZnO/Al_2O_3 is a solid acid catalyst. Thus, Na or K would form much stronger bond with the surface of CuZnO/Al_2O_3 than CuZnO/MgO.

From Figure 4.14, the refined glycerol mixed with 0.1% Na exhibited the highest conversion, followed by the refined glycerol mixed with 0.1% K and the refined glycerol, respectively. This could be because the Na and K might hardly deposit on CuZnO/MgO, as shown in Table 4.6, and the addition of Na or K increased the pH value to the refined glycerol feedstock, as shown in Table 4.8. The higher pH value of the reaction solutions on glycerol hydrogenolysis led to the more glycerol conversion and propylene glycol selectivity (Wang *et al.*, 2007).

Table 4.6 Concentration of alkali on feedstock, product, and the spent $CuZnO/Al_2O_3$ and CuZnO/MgO catalysts analyzed by AAS

Catalyst	Feedstock	Feedstock (ppm)	Product (ppm)	Spent catalyst (ppm)
$CuZnO/Al_2O_3$	Refined glycerol + 0.1%Na	1,010	1,091	110
	Refined glycerol + 0.1%K	1,081	1,071	139
CuZnO/MgO	Refined glycerol + 0.1%Na	976	979	3
	Refined glycerol + 0.1%K	991	1001	1

From Figures 4.15-4.16, the decreasing of propylene glycol selectivity led to the increasing of acetol selectivity. The results agreed well with the mechanism proposed by Dasari *et al.* (Dasari, M.A., 2005) as shown in Figure 4.8.

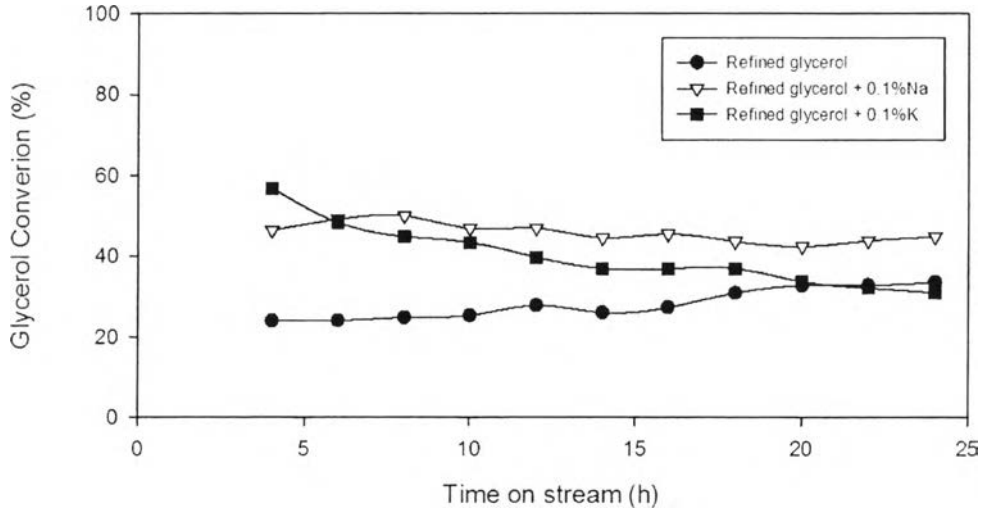

Figure 4.14 Plot of glycerol conversion as a function of time on stream over CuZnO/MgO on different impurities in the glycerol feedstock (Reaction conditions: 80wt% glycerol feed, 250 °C, 500 psig, H_2:glycerol = 4:1, and WHSV = 3.77 h^{-1}).

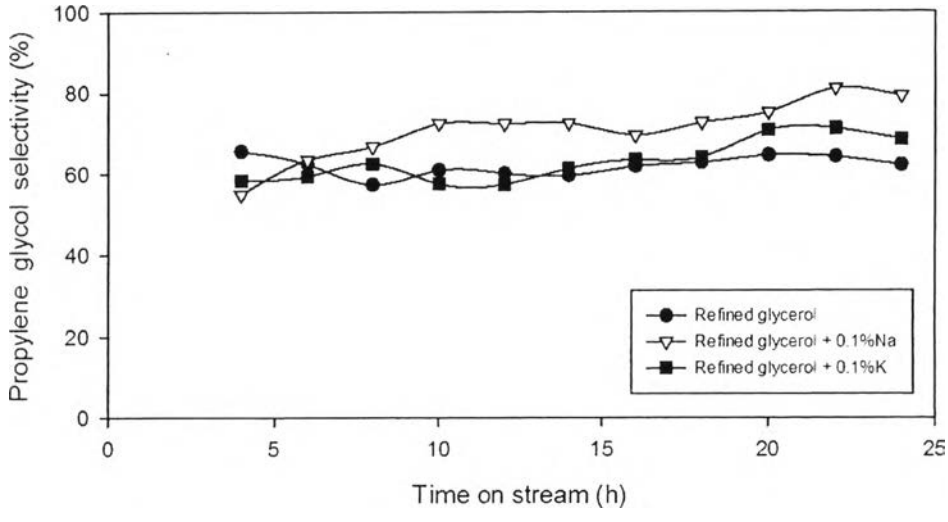

Figure 4.15 Plot of selectivity to propylene glycol as a function of time on stream over CuZnO/MgO on different impurities in the glycerol feedstock (Reaction conditions: 80wt% glycerol feed, 250 °C, 500 psig, H_2:glycerol = 4:1, and WHSV = 3.77 h^{-1}).

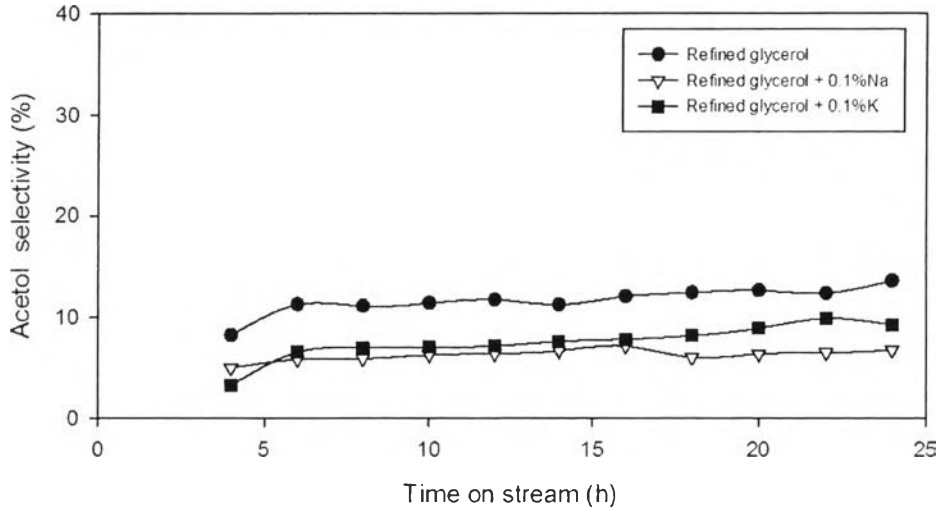

Figure 4.16 Plot of selectivity to acetol intermediate as a function of time on stream over CuZnO/MgO on different impurities in the glycerol feedstock (Reaction conditions: 80wt% glycerol feed, 250 °C, 500 psig, H_2:glycerol = 4:1, and WHSV = 3.77 h^{-1}).

Table 4.7 Conversion and selectivity to liquid products of CuZnO/MgO on different impurities in the glycerol feedstock (Reaction conditions: 80wt% glycerol feed, 250 °C, 500 psig, H_2:glycerol = 4:1, WHSV = 3.77 h^{-1}, and TOS of 24 h)

Catalysts		**Refined glycerol**	**Refined glycerol + 0.1%Na**	**Refined glycerol + 0.1%K**
Conversion (wt. %)		29.88	45.06	31.14
Selectivity to liquid products (wt. %)	Acetone	1.93	1.54	1.61
	2-propanol	0.99	-	-
	Acetol	9.78	6.68	9.20
	Propylene Glycol	64.29	78.32	67.78
	Ethylene Glycol	4.13	3.79	3.54
	Others	18.88	9.67	17.87

Table 4.8 pH value analyzed by pH-indicator strips

Feedstock	**pH**
Refined glycerol	7
Refined glycerol + 0.1%Na	11
Refined glycerol + 0.1%K	11

The TPO profiles and the calculated amounts of carbon deposition on the spent CuZnO/MgO catalyst on different impurities in the glycerol feedstock —the refined glycerol, the refined glycerol mixed with 0.1% Na, and the refined glycerol mixed with 0.1% K are shown in Figure 4.17. The results show that the spent catalyst of the refined glycerol as feedstock contained the highest amount of coke deposition on the catalyst surface compared to the spent catalyst of refined glycerol mixed with 0.1% Na and with 0.1% K. This could be because the higher pH value of the reaction solutions on glycerol hydrogenolysis led to the more glycerol conversion and propylene glycol selectivity (Wang *et al.*, 2007). Thus, the higher pH value might reduce coke.

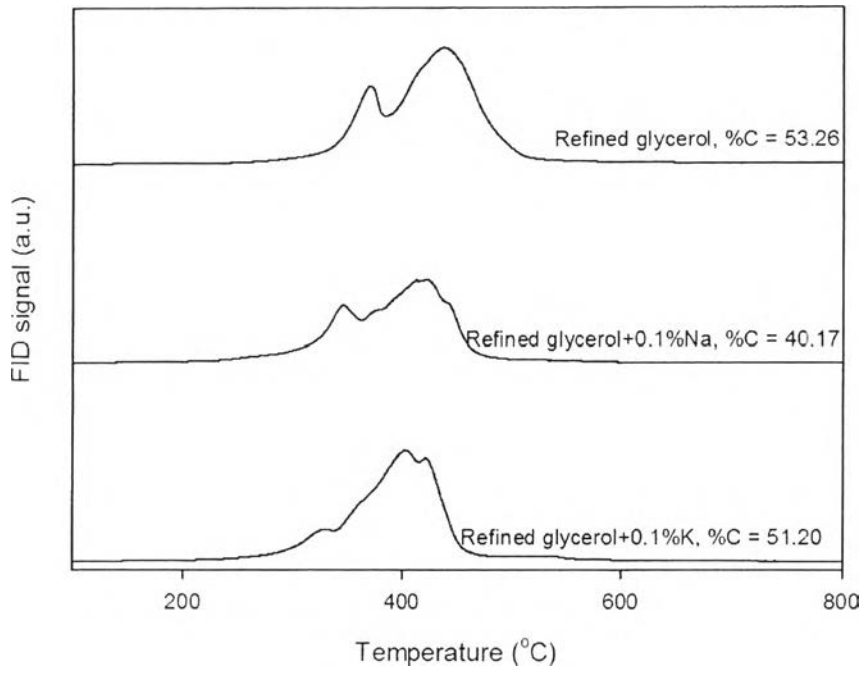

Figure 4.17 TPO profiles of CuZnO/MgO on different impurities in the glycerol feedstock after 24 h TOS (Reaction conditions: 80 wt% glycerol feed, 250 °C, 500 psig, H_2:glycerol = 4:1, and WHSV = 3.77 h^{-1}).

4.3 Catalyst Deactivation and Catalyst Regeneration

4.3.1 Coke Formation

Noticeably, CuZnO/MgO exhibited the highest performance in terms of stability compared to the other prepared catalysts. Nevertheless, the coke formation of CuZnO/MgO was very high so the coke profile was further investigated as shown in Figure 4.18. The result shows that the coke percentage increased considerably in the first four hour time on stream and gradually increased after that. This high amount of coke might hinder the active site of the catalyst, thereby, the catalytic activity was low.

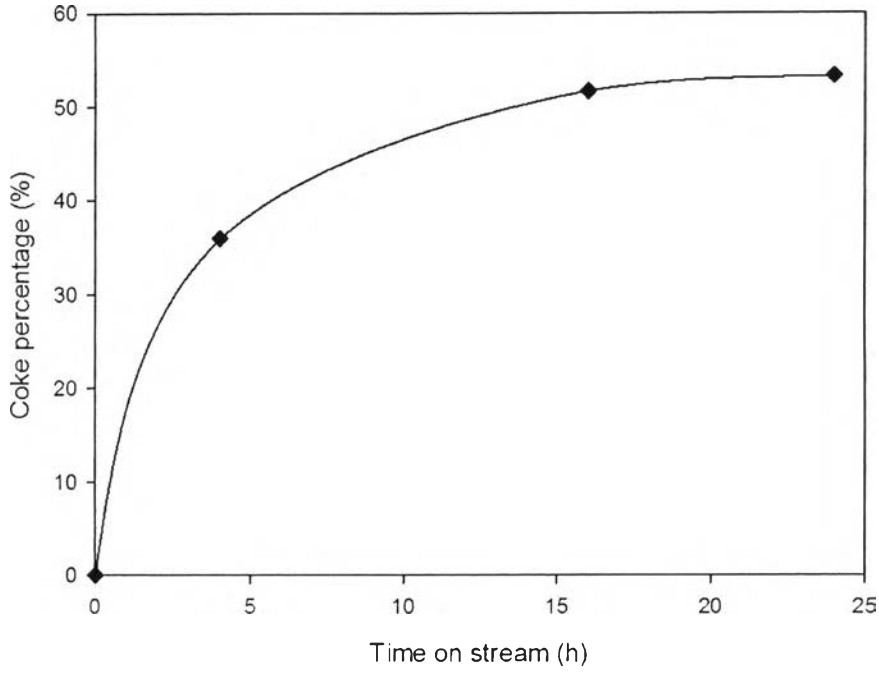

Figure 4.18 Coke profile of CuZnO/MgO as a function of time on stream (Reaction conditions: 80wt% glycerol feed, 250 °C, 500 psig, H_2:glycerol = 4:1, and WHSV = 3.77 h^{-1}).

4.3.2 Catalyst Regeneration

The highest performance in terms of stability compared to the other prepared catalysts was CuZnO/MgO. Thus, the spent CuZnO/MgO catalyst was regenerated in-situ in this study in order to eliminate the deposited coke on the catalyst surface. Then the regenerated CuZnO/MgO catalyst was tested for its activity in the same condition as the fresh catalysts.

From Figure 4.19, the glycerol conversion of the regenerated CuZnO/MgO catalyst was as good as the fresh CuZnO/MgO catalyst. From Figures 4.19 and 4.20, the regenerated CuZnO/MgO catalyst gave higher selectivity to propylene glycol and less selectivity to acetol than the fresh CuZnO/MgO catalyst. The carbon deposit on the regenerated CuZnO/MgO catalyst was less than the fresh CuZnO/MgO catalyst, as shown in Figure 4.22.

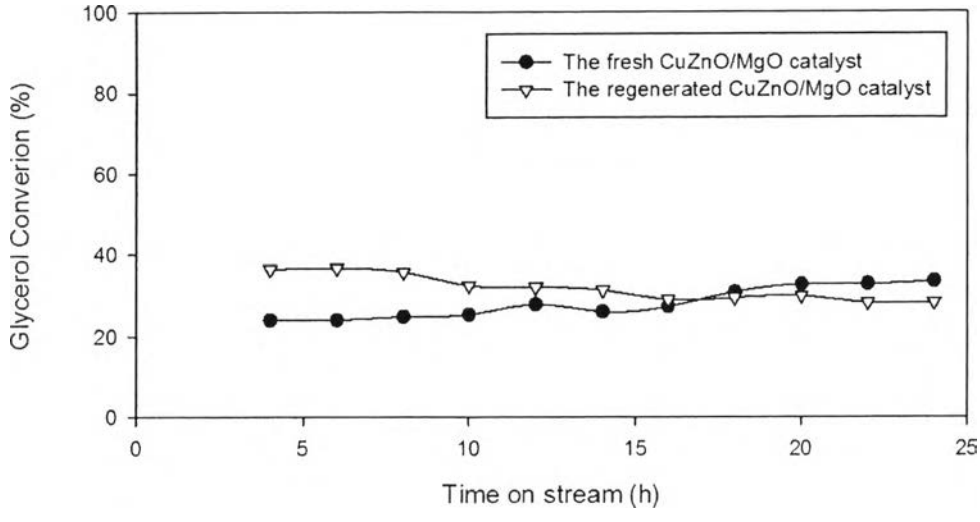

Figure 4.19 Plot of glycerol conversion as a function of time on stream of the fresh and regenerated CuZnO/MgO catalysts (Reaction conditions: 80wt% glycerol feed, 250 °C, 500 psig, H_2:glycerol = 4:1, and WHSV = 3.77 h^{-1}).

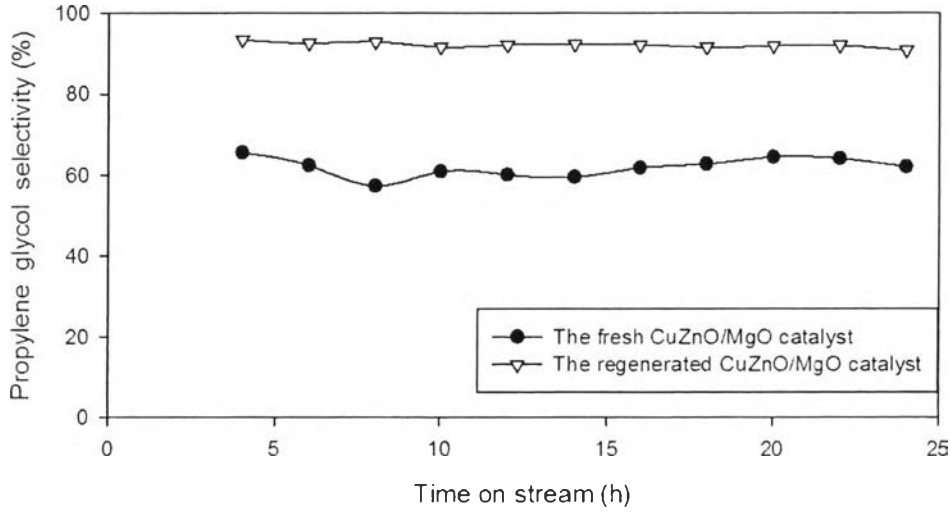

Figure 4.20 Plot of selectivity to propylene glycol as a function of time on stream of the fresh and regenerated CuZnO/MgO catalysts (Reaction conditions: 80wt% glycerol feed, 250 °C, 500 psig, H_2:glycerol = 4:1, and WHSV = 3.77 h^{-1}).

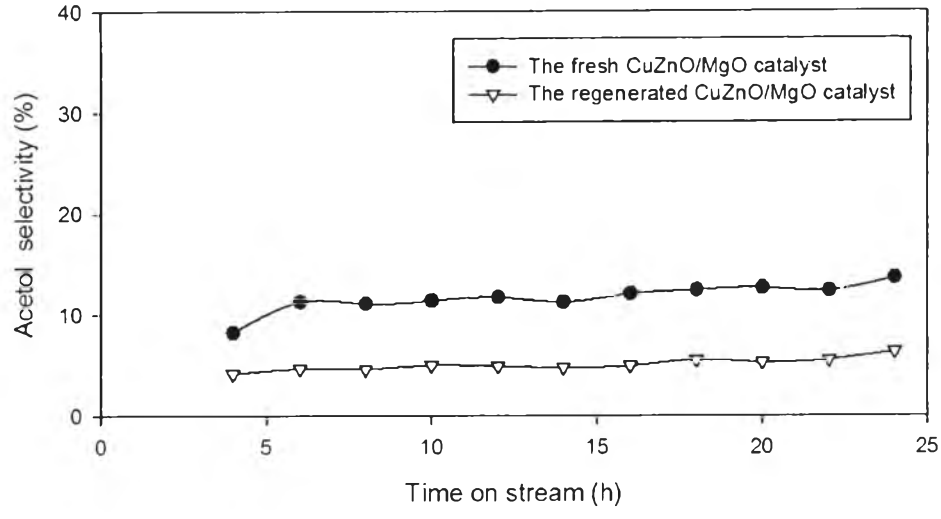

Figure 4.21 Plot of selectivity to acetol intermediate as a function of time on stream of the fresh and regenerated CuZnO/MgO catalysts (Reaction conditions: 80wt% glycerol feed, 250 °C, 500 psig, H_2:glycerol = 4:1, and WHSV = 3.77 h^{-1}).

Table 4.9 Conversion and selectivity to liquid products of the fresh and regenerated CuZnO/MgO catalysts (Reaction conditions: 80wt% glycerol feed, 250 °C, 500 psig, H_2:glycerol = 4:1, WHSV = 3.77 h^{-1}, and TOS of 24 h)

Catalysts		**Fresh CuZnO/MgO**	**Regenerated CuZnO/MgO**
Conversion (wt. %)		29.88	19.42
Selectivity to liquid products (wt. %)	Acetone	1.93	-
	2-propanol	0.99	-
	Acetol	9.78	6.21
	Propylene Glycol	64.29	89.07
	Ethylene Glycol	4.13	4.72
	Others	18.88	-

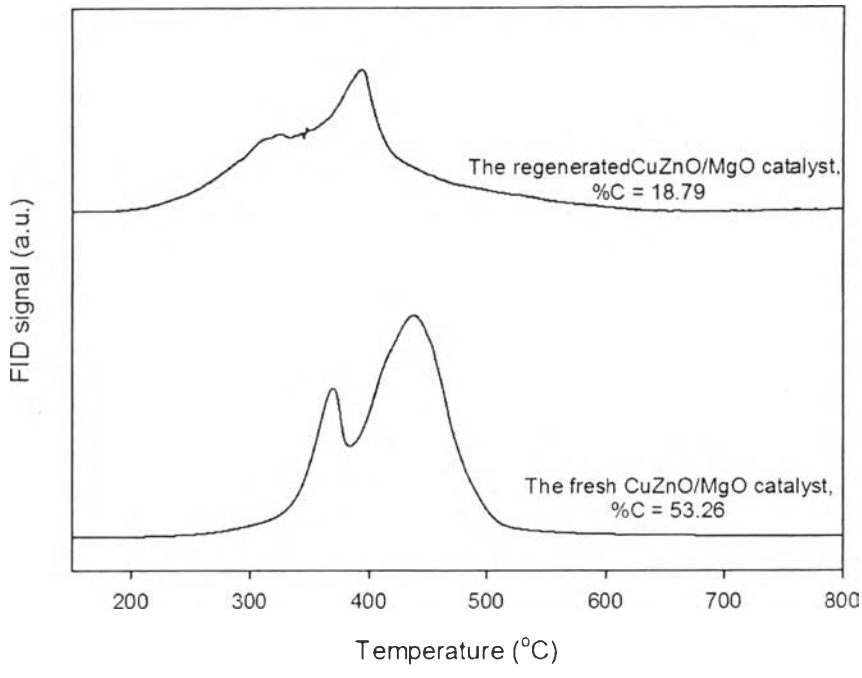

Figure 4.22 TPO profiles of the fresh and regenerated CuZnO/MgO catalysts after 24 h TOS (Reaction conditions: 80wt% glycerol feed, 250 °C, 500 psig, H_2:glycerol 4:1, and WHSV = 3.77 h^{-1}).

Figure 4.23 exhibits the XRD patterns of the fresh and regenerated CuZnO/MgO catalysts. The results showed that CuO (2θ of 35.6° and 38.8°) peak of the regenerated CuZnO/MgO catalyst was sharper than the fresh catalyst. This could be because the regenerated CuZnO/MgO catalyst had larger crystalline size of CuO than the fresh catalyst. In addition, the TPR profiles of the fresh and regenerated CuZnO/MgO catalysts are shown in Figure 4.24. The reduction peak of the regenerated CuZnO/MgO catalyst was shifted to higher temperature, compared to the fresh catalyst. This could be because the primary particles would aggregate to form the larger grains of particles (Tang *et al.*, 2009). From Table 4.1, the BET surface areas of the fresh and regenerated CuZnO/MgO catalysts were 24 and 31 m^2/g, respectively. Moreover, the regenerated CuZnO/MgO had more small pores than the fresh catalyst, as shown in Figure 4.1 e. The larger crystalline size of CuO and the higher surface area of the regenerated CuZnO/MgO catalyst, compared to the fresh catalyst, might be the reason of the regenerated CuZnO/MgO catalyst gave higher

selectivity to propylene glycol and less selectivity to acetol than the fresh CuZnO/MgO catalyst.

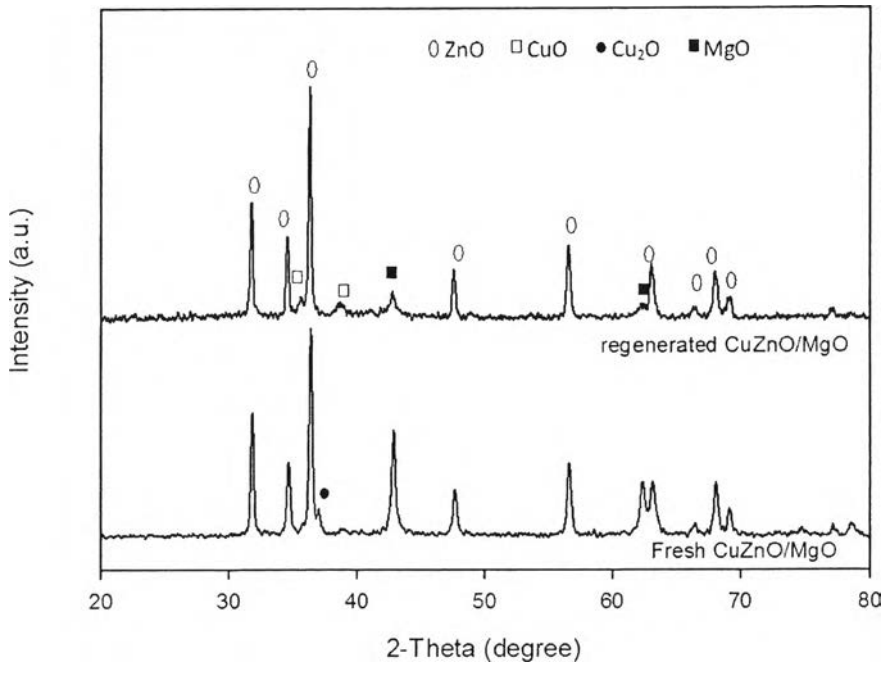

Figure 4.23 XRD patterns of the fresh and regenerated CuZnO/MgO catalysts.

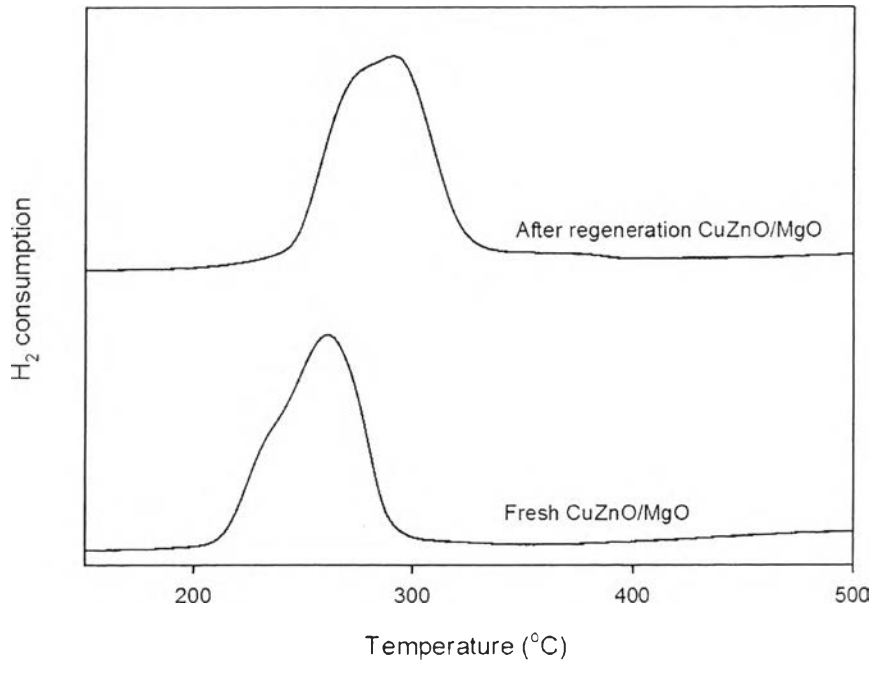

Figure 4.24 TPR profiles of the fresh and regenerated CuZnO/MgO catalysts.